Development of an open hardware bioreactor for optimized cardiac cell culture integrating programmable mechanical and electrical stimulations

Cite as: AIP Advances **10**, 035133 (2020); https://doi.org/10.1063/1.5144922
Submitted: 12 January 2020 . Accepted: 05 March 2020 . Published Online: 31 March 2020

Jonathan Béland, James Elber Duverger, Estelle Petitjean, Ange Maguy, Jonathan Ledoux, and Philippe Comtois

Development of an open hardware bioreactor for optimized cardiac cell culture integrating programmable mechanical and electrical stimulations

Cite as: AIP Advances 10, 035133 (2020); doi: 10.1063/1.5144922
Submitted: 12 January 2020 • Accepted: 5 March 2020 •
Published Online: 31 March 2020

Jonathan Béland,[1,2] James Elber Duverger,[1,3] Estelle Petitjean,[1] Ange Maguy,[1,4] Jonathan Ledoux,[1,2,5] and Philippe Comtois[1,2,3,a)]

AFFILIATIONS

[1]Research Center, Montreal Heart Institute, Montreal, Quebec H1T 1C8, Canada
[2]Department of Pharmacology and Physiology, Université de Montréal, Montreal, Quebec H3T 1J4, Canada
[3]Institute of Biomedical Engineering, Université de Montréal, Montreal, Quebec H3T 1J4, Canada
[4]Department of Physiology, University of Bern, CH-3012 Bern, Switzerland
[5]Department of Medinine, Universite de Montreal, Quebec, Canada

[a)]**Current address:** Research Centre, Montreal Heart Institute, 5000 Belanger E., Montreal, Quebec, H1T 1C8, Canada. **Author to whom correspondence should be addressed:** philippe.comtois@umontreal.ca. **Telephone:** 514-376-3330 **ext.** 2615

ABSTRACT

A new open-hardware bioreactor capable of applying electrical field stimulation in conjunction with static or cyclic stretch is presented. Stretch is applied to cells by a specially designed elastomeric membrane with a central seeding region. The main interest of our approach is the fine control of the characteristics of stimulations in regard to timing and amplitude in a simple design based on affordable, easy to find components and 3D printable parts. Our approach opens the way to more complex protocols for electrical and/or mechanical stimulations, which are known important regulators of cardiac phenotypes.

INTRODUCTION

Even after huge improvement in prevention and therapies, which have been causing mortality rates to decline significantly since 1980,[1] cardiovascular disease remains a major cause of death, many attributable to ischemic heart disease. Although great developments have been made, there is a need for novel and individualized therapeutic strategies, e.g., disease-specific or patient-specific drugs, and cardiac tissues for regenerative medicine. To be able to produce an optimal cardiac replacement tissue, we need to understand the link between the engineered tissue physiology and its environment. From a physiological point of view, the heart is an organ that pumps the blood and allows its propulsion throughout the entire vascular system. These functions are determined by a precise combination of electrical and mechanical activation of the cardiac cells. These cells are under the constant influence of diverse stimuli, necessitating unceasing adaptation to the constraints of their environment. Recent advances in the field of stem cell biology[2,3] and cardiac tissue engineering[4,5] have led to the development of human cardiac tissues highly similar to native, non-engineered tissues. These tissues have shown potentials to be used as a physiologically relevant substrate for investigations and drug testing platforms.[6] However, use of these tissues for discovery implies that their phenotype must be consistent with the pathological/physiological tissue sought.

There is strong evidence in the literature that cardiac cells *in vitro* need to be grown in a controlled environment incorporating a combination of coordinated electrical[7–9] and mechanical[10,11] stimulations for optimized physiological functions of contractile engineered tissue.

Different types of materials have been used as electrodes for electrical stimulation: silver–silver chloride,[12,13] titanium,[9,14] titanium-nitride,[9] stainless steel,[13] hydrogel,[13] platinum,[15–17] and platinum–iridium,[18] but carbon electrodes[9,19–21] appear to be the best option currently available.[9,19,22] Carbon electrodes offer a much greater resistance than metal,[13] exhibit the best charge transfer characteristics and the lowest percentage of injected charge unrecovered, and, thus, constitute an excellent material for a bioreactor.[9] In general, electrical stimulations can be applied in two ways (local and field stimulation) although other approaches including optogenetics are being evaluated.[23] Local stimulation aims at injecting current to a precise location of the extra- or intracellular environment with the use of electrodes (unipolar or bipolar) that will activate local cells; the localized activation (with a minimum of depolarized cells) then propagates to all connected cells.[24] Field stimulation aims at depolarizing all cells within the culture by the application of an electric field issued from the voltage between two parallel electrodes. Field stimulation is preferable for cell culture stimulation protocols since both isolated cells (or cell islands) and connected syncytium can be stimulated simultaneously. It is worth noting that the electrode length should be greater than twice the distance between the electrodes. In addition, a stimulus of 5 V/cm should be used, according to the maximal stimulation amplitude of 8 V/cm previously established.[9] Field stimulation tends to improve the alignment of the cells because charges in the cytosol will act as a dipole and align in the direction of the field.[25]

In the culture, cells are sensitive to the presence or absence of electrical stimulation. The presence of electrical stimulation will improve the geometry, alignment of the sarcomeres, and distribution of connexin-43 (Cx-43, cell-to-cell communication) and the mitochondria (energy).[21,26,27] Two types of pulses can be used to apply the electrical stimulation: monophasic or biphasic pulses. Both types of pulses can increase Cx-43 expression/localization, but biphasic pulses are more efficient.[27] Biphasic pulses also upregulate cardiac transcription factors such as MEF2D, GATA-4, and Nkx2.5 as well as the expression of sarcomeric proteins, troponin T, alpha-actinin, and SERCA 2a in human progenitor cells.[27] On the other hand, the absence of electrical stimulation will lead to round-shaped cells as well as the remodeling of actin and troponin-I, leading to diminished contractile properties.[28] From a functional point of view, cardiomyocytes under the influence of the electrical stimulation will display a greater number of synchronized contractions, a higher entrainment frequency,[26] and less hypertrophy.[29] Electrical stimulation helps in the formation of regular activity (contractions), promoting then an optimized intracellular calcium handling,[30] density, and function of the L-type calcium channel.

The mechanical environment plays an important role in cardiomyocyte function and, therefore, is inherent to the physiological development of the heart or cardiac pathologies.[31] Cardiomyocytes are subject to extreme dynamic changes in terms of stress and strain[32] and therein, are ideal targets to study stretch related conditions. The electrical activity of a cardiomyocyte is directly linked with its mechanical activity through the excitation–contraction coupling principle. The presence of a mechanical–electrical feedback is also emerging as a key modulator of both cellular and tissue electrophysiological properties.[33] For example, acute stretching activates channels that alter cardiac automaticity, evoking depolarizing currents in cardiomyocytes (entry of calcium and sodium). The entry of calcium enhances the influx of sodium by the sodium–calcium exchanger and can lead to the formation of the action potential.[34] Acute stretch is known to decrease the cardiac conduction velocity as a function of the stretch level and orientation relative to impulse propagation.[35] Interestingly, chronic stretch can also modulate the electrical propagation by increasing Cx-43 expression, then leading to an increase in the conduction velocity.[36]

To mimic the mechanical environment of the cardiac cells, the use of pressure variation or motors is required to apply a deformation to the substrate.

We aim at developing a bioreactor (BioR) to optimize *in vitro* development of cardiac replacement tissues. We describe here our BioR and characterize the impact of electrical field stimulation and mechanical stimulation, applied individually or combined, on neonatal rat cardiomyocyte physiology.

METHOD

Characterization of electrical and mechanical sub-systems

Data for the evaluation of the electrical stimulation sub-system were acquired using NI USB-6221 DAQ (National Instruments, Inc., USA) controlled by a custom *Python* program using the PyDAQmx library. Acquisitions were sampled at 10 kHz to test the period of stimulation and at 100 kHz to evaluate the bipolar stimulation duration.

Data for the evaluation of the mechanical stimulation sub-system were acquired using a large field universal serial bus (USB) camera (Dino-Lite, Taiwan). Images at different displacements of the motors were acquired to estimate the deformation of the seeding template. Video recordings (frame rate of 15 fps) were acquired and analyzed using Matlab to validate the temporal period of cyclic stretch.

Tests with cells in the BioR were done in a Thermo Forma Series II incubator kept at 37 °C with 5% CO_2.

Cardiomyocyte isolation procedure

All animal-handling procedures were in concordance with the Canadian Council on Animal Care guidelines and were approved by the institutional animal research ethics committee. Cardiomyocyte isolation was performed according to the protocol of the neonatal cardiomyocyte isolation kit from Worthington. In summary, 1 to 3 day old rats (Sprague–Dawley, Charles River) were killed by decapitation. Beating hearts were removed from the rats and immediately put in cold Ca^{2+} and Mg^{2+}-free Hank's Balanced Salt Solution. Ventricular muscle was selected by excision, and tissue was minced on ice into 1–3 mm^3 pieces. The mixture was subjected to purified enzymatic digestion (trypsin and collagenase). Isolated cells (enriched cardiomyocytes) were counted and seeded at a density of 6.5×10^5 cells/cm^2 in the seeding area of the membrane pre-coated with 0.2% porcine-derived gelatin (G1890, Sigma) and 0.001 25% fibronectin solution (F1141, Sigma). Cells were grown for 48 h in Dulbecco's Modified Eagle's Medium (DMEM, 319-050-CL, Wisent) with 10% fetal bovine serum (SH30396.03, Fisher Scientific Co. Ltd.) and 1% penicillin/streptomycin (450-201-EL, Wisent). A concentration of 100 μg/ml of Normocin (ANT-NR-1, InvivoGen) was used in a subset of experiments. Fetal bovine serum was then reduced to 5%

in DMEM with 1% penicillin/streptomycin to limit the impact of hypertrophy.

HEK239t cell culture

HEK293t was used to test adhesion of cultured cells during deformation of the flexible culture template within the BioR. Briefly, amplification of the HEK293t into a 100 mm^2 cell culture dish is continued until approximately 90% confluence is obtained by changing the complete DMEM media (10% fetal bovine serum and 1% penicillin/streptomycin) every 3 days. Then, cells were detached from the Petri dish using a mixture of trypsin/ethylenediamine tetraacetic acid (EDTA) 1× (5 min at 37 °C). Cells were then seeded on the membrane template (5×10^5 cells/ml) in the BioR. Cells were rested for 24–48 h prior experimentation to ensure optimal adhesion and density.

Fluorescence of calcium dynamics

Calcium transients were recorded to evaluate the electrical stimulation sub-system. After 5 days of culture, cardiomyocytes were washed with fresh media and incubated with 10 μM of fluo-4 AM (*F-14201*, *Life technologies*, *Burlington*, *ON*, *Canada*) and 0.2% pluronic acid F-127 (P-3000 MP, Life Technologies) for 30 min at 37 °C. Fluo-4-loaded cardiomyocytes were then washed four times with fresh phenol-red-free media, followed by a 15 min resting period to allow de-esterification of the dye. Calcium transient mapping experiments were performed in phenol-red-free DMEM, at 37 °C. Fluorescence was recorded for 30 s at 125 Hz with a CardioCCD camera (RedShirt Imaging, Decatur, GA, USA). The dye was excited with a quartz tungsten halogen lamp (*Oriel Instruments Inc.*, *Stratford*, *CT*). The filters used for excitation and emission were $\lambda_{excitation} \approx 480 \pm 20$ nm (*Chroma Technology Corp*, *Bellows Falls*, *VT*) and $\lambda_{emission} \approx 535 \pm 25$ nm (*Semrock, Inc.*, *Rochester*, *NY*), respectively. Signals were filtered and analyzed using an in-house program using Matlab software (*R2008*, *MathWorks, Inc.*, *Natick*, *MA*).

SYSTEM DESCRIPTION AND RESULTS

Physical design of the bioreactor

The 3D layout of the BioR is presented in Fig. 1. The key components of the system are highlighted and include the items needed for the mechanical and electrical stimulation. BioR is designed around a "safe for food" crystal clear polystyrene disposable and recyclable enclosure (4 1/4″ × 1 1/2″ unhinged container, Gary Plastic Packaging Corp., NY), which sits on a custom-made Lexan support with two linear stepper motors (Haydon 28000 Series size 11 ID 7, Haydon Kerk Motion Solutions, Inc.). These motors have a step size of 3.175 μm at full step. Each motor is physically connected to a 3D printed acrylonitrile butadiene styrene (ABS) membrane support that transfer the shaft translation to an elongation of the polydimethylsiloxane (PDMS) membrane on which adherent cells are cultured. The displacement is restricted along the lengthiest dimension of the enclosure and guided by two parallel 17-4 PH stainless steel rods (diameter = 2.38 mm, length = 101.6 mm, McMaster-Carr, Inc.). The rods are anchored in a 3D printed ABS frame (bottom left inset of Fig. 1), which also houses the carbon electrodes (dimensions: 3.175 mm × 6.35 mm 96.164 mm, SK-05 ISO Graphite Plates, Industrial Graphite Sales LLC) for electrical stimulation. The BioR is compatible with cell culture within an incubator. All electronics except the motors and the carbon electrodes are located outside the incubator.

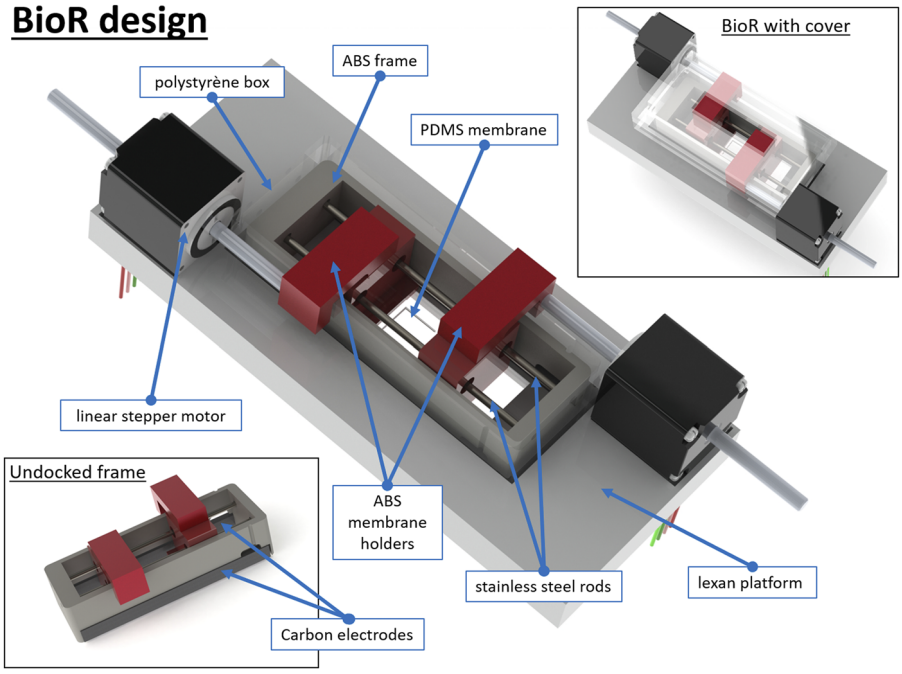

FIG. 1. Overall design of the bioreactor showing the mechanical and electrical stimulation sub-systems. The mechanical stimulation is applied to the cells attached to a homemade PDMS membrane through elongation of the membrane. Stretch of the membrane is done by the controlled displacement of two motor shafts. The displacement is constrained along two stainless steel rods by the movement of 3D printed membrane ABS holders. The stainless steel rods are held in place by an ABS frame, which also serves to stabilize the carbon electrodes for electrical stimulation. Bottom left inset: Schematic of the frame showing the carbon electrode positions and membrane holders. The membrane holders have Teflon cylindrical inserts through which stainless steel rods pass through for decreased resistance to movement. Upper right inset: The bioreactor is shown with the transparent cover to allow direct imaging techniques.

PDMS membrane and culture seeding area

A polydimethylsiloxane (PDMS)-based cell culture membrane was used considering that the mechanical properties are easily modulated within physiologically relevant ranges[37] and it is resistant to mechanical deformations. PDMS is also biocompatible and easy to use[38] as well as transparent. Cells were cultured on an elastomeric PDMS (SYLGARD 184, Dow Corning) membrane that was designed with T-shaped ends to be held by the membrane supports and a center depressed region for cells (see Fig. 2 for details on dimensions). An aluminum mold was designed using Solidworks (Dassault Systems Corp.), where parts A and B were designed and machined (left insets of Fig. 2) with an open top to let air bubbles escape from the mold. Degassing was performed before injecting the PDMS into the mold with a vacuum pump (Platinum DV-85N, JB Industries). The degassed binary compound (a mixture of a base and curing agent) was injected through a luer-lock tip hole. A ratio of compounds (curing agent:base) of 1:20 was used as this ratio has a Young's modulus similar to physiological cardiac tissue while still being easy to handle.[39]

Electronic control module for electrical and mechanical stimulation

The prototype was built with a central microcontroller to control the timing of both the electrical and mechanical stimulation subsystems, as shown in Fig. 3. An Arduino Mega 2560 (Arduino.cc) has been chosen for faster and more accessible development. Additionally, this variant of prototyping Arduino boards offers more digital outputs in comparison with the UNO or other smaller boards. These additional digital outputs are needed to drive both electrical and mechanical sub-systems. The microcontroller within the Arduino is an ATmega2560 with 256 KB of flash memory (of which 8 KB is used for the bootloader), 8 KB of static random access memory (SRAM), and 4 KB of electrically erasable/programmable read-only memory (EEPROM).

Characteristics of the electrical stimulation sub-system

The timing and waveform of the electrical stimulation were driven by the microcontroller, which changes the digital output of pins 46–53 to modulate the output of the 8-bit digital-to-analog converter (TLC7226CDW, Texas Instruments), as shown in Fig. 3. A power operational amplifier (LM675T, Texas Instruments) was used with 5 W resistors R1 and R2 to form a non-inverting amplifier configuration. The gain (×3.33) of the amplification increases the output from the level selected by the user using a scaling factor in the code. The electric field is applied to the cells via a pair of parallel carbon plate electrodes [depicted in Fig. 4(a)]. The system allows voltage amplitudes up to ±16 V. The current is limited to 250 mA by the resistance R3 (in series with the cell culture setup resistance, as seen Fig. 3).

Electrical stimulation protocol

The electrical stimulation is based on field stimulation with a voltage difference applied to the cells via carbon electrodes [schematically shown in Fig. 4(a)]. A biphasic stimulation waveform, with sequential positive/negative polarities per pulse, was chosen to decrease accumulation of charges at the electrodes. Temporal resolution of the stimulation is of the order of the microseconds. Examples of output measured at R3 are shown in panel (b) for a combined t_{stim} ms up and t_{stim} ms down square pulses (set

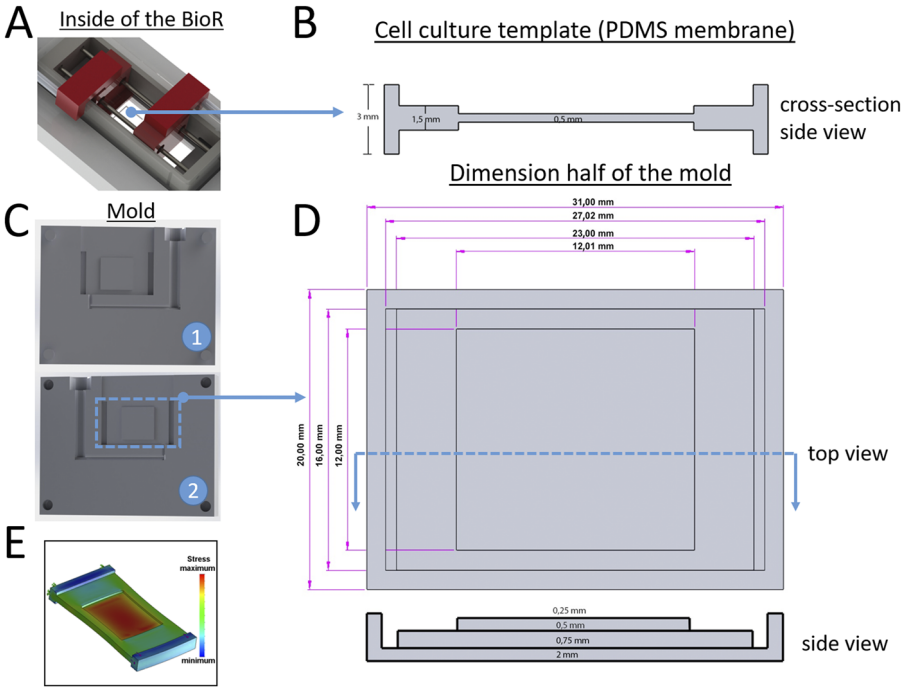

FIG. 2. Characteristics of the homemade PDMS cell culture template (all dimensions are in mm). (a) Close-up of the membrane in the bioreactor where the cells are cultured. (b) Cross section of the PDMS membrane showing the side T morphology for anchoring to the membrane holder. The thinner section in the middle corresponds to the area where cells are seeded. (c) The membrane is created by the molding technique with a symmetric two-part mold (part 1 and 2). (d) Dimensions of one part of the mold. (e) Simulated spatial dispersion of the stress when elongation is applied along the length of the membrane showing that the maximum stress is found within the seeding region (red regions of the membrane).

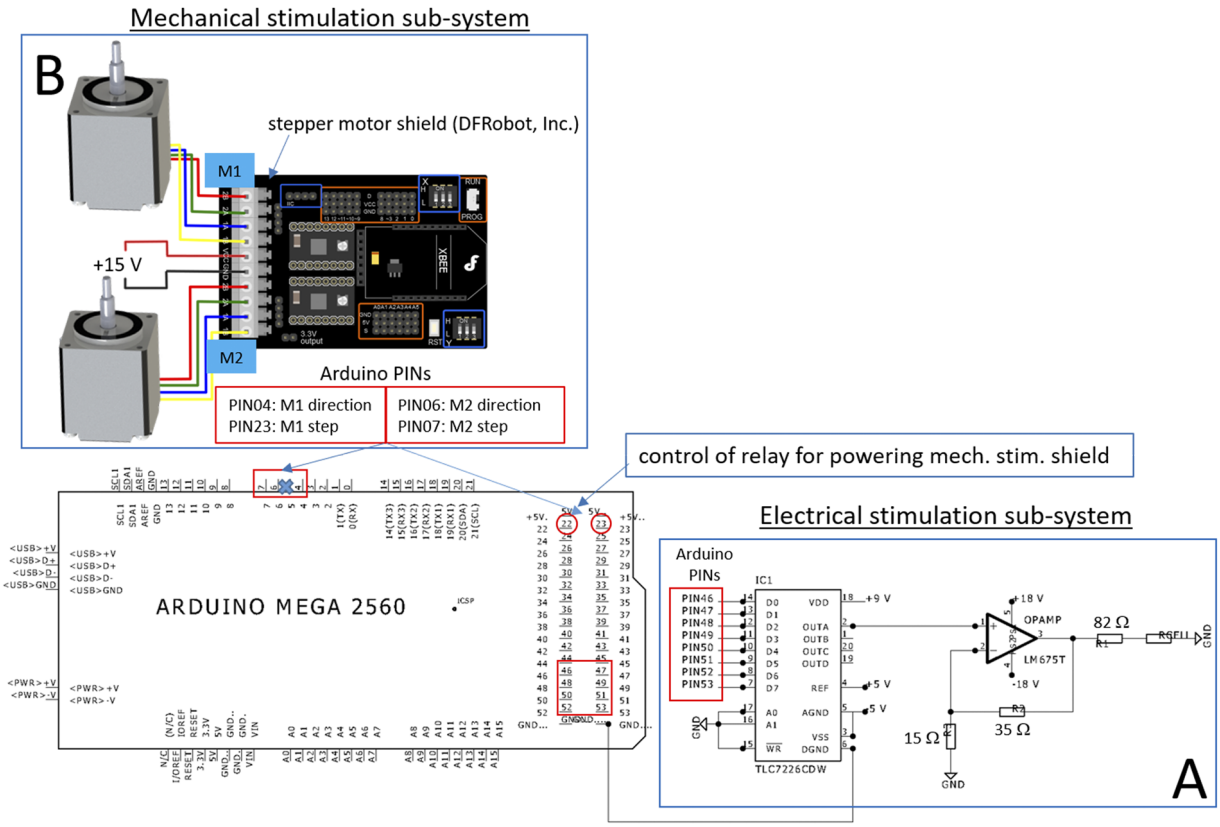

FIG. 3. Details of the bioreactor electronic components for the mechanical and electrical sub-systems that are both controlled by the Arduino MEGA board. Inset (a): Electrical stimulation sub-system showing the digital-to-analog converter with the output from port A feeding the non-inverting amplifier circuit. Inset (b): Schematic of the shield and connection that controls the linear stepper motor movement.

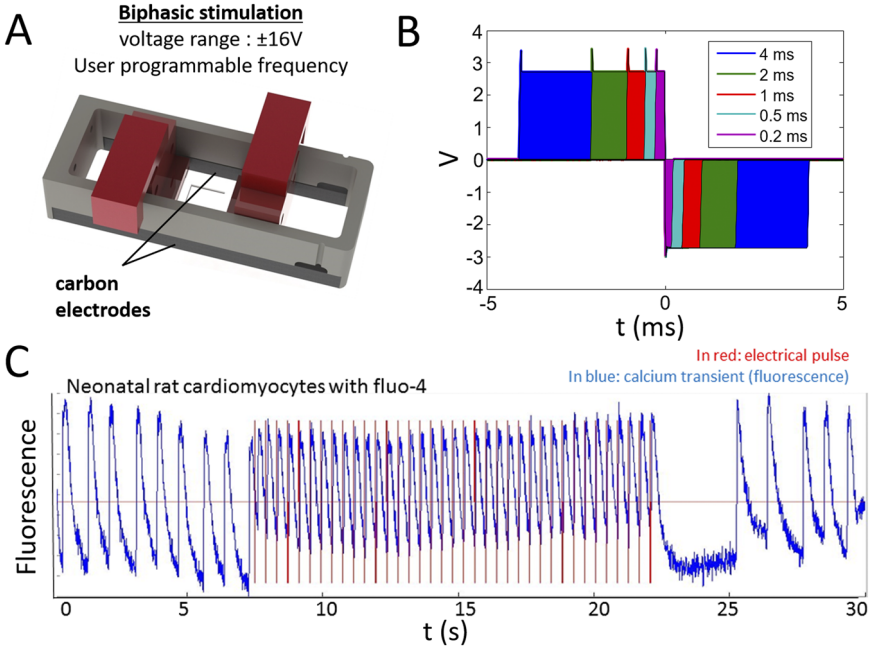

FIG. 4. Electrical stimulation. (a) The electrical stimulation in the bioreactor is applied by field stimulation with a maximum voltage amplitude of 16 V in both polarities. The voltage difference is applied to the cells cultured between the two carbon electrodes. (b) Typical outputs measured at resistor R1 (current limited resistor) showing the bipolar stimulation with positive and negative pulses (stimulation duration per phases shown are 0.2 ms, 0.5 ms, 1.0 ms, 2.0 ms, and 4.0 ms as presented in the legend). Duration of the pulses can be modified by the user. (c) Calcium transients of cardiomyocytes (Fluo-4 fluorescence shown in blue) before, during, and after pacing (pacing voltage shown in red). A clear entrainment of the cells is shown at a pacing frequency of 2.5 Hz (stimulation characteristics of 2 ms per polarity and amplitude of 10 V/cm).

of t_{stim} shown in the legend). However, these stimulation characteristics can be modified as long as the up + down voltage total duration is less or equal to the pacing cycle length defined by the user. The benefit of the proposed design is that a variety of stimulation protocols can be implemented. For example, unipolar (with positive or negative polarity) or alternating output (a different bipolar stimulation with alternation between positive and negative outputs) could be programmed. The timing of the voltage changes is set by modifying the 8-bit digital output of the Arduino intrinsic timer using interrupt functions from the TimerOne library (http://github.com/PaulStoffregen/TimerOne). The timer is configured to repetitively measure a period of time, in microseconds. At the end of each period, an interrupt function runs to modify the 8-bit digital output of the Arduino controlling the DAC state and output voltage. Output to the amplification circuit can be set to ground via an analog switch for safety purposes. The comparison between the programmed period of stimulation (T) and the mean measured T is linear with same values for a given T [see Fig. 5(a)]. The inset in the panel shows that the standard deviation of T calculated for different periods of stimulation is less than 0.1 ms. Examples for T = 1000 ms, 500 ms, and 200 ms are plotted in Fig. 5(b).

An example of bipolar stimulation of cardiomyocyte is depicted in Fig. 4(c). Cells were grown on the substrate for 5 days prior to the initiation of the electrical stimulation protocol, which consisted of 2 ms pulses of 4.5 V/cm at 1 Hz.

Characteristics of the mechanical stimulation sub-system

The system was designed with the stepper motor shield (DFRobot, Inc.), which can drive both linear stepper motors of the BioR and induce deformation of the elastic template [Fig. 6(a)] using only two digital outputs from the Arduino (as depicted in Fig. 3) for each motor. Simultaneous retraction of the motors stretches the membrane, while the forward movement reverts the stretch level to the initial state. An example of stretched cells cultured on the PDMS template is shown in Fig. 6(c). Approximately, 14% stretch was applied in this example.

Power to the shield and motors is controlled using a relay board (model 3051, Phidgets, Inc.), which is digitally controlled through the Arduino pin 22. The shield is based on the Polulu A4988 chips (one per motor). Digital outputs for each motor determined the direction and the timing of steps. Usually, pin 4 (direction) and pin 5 (stepping) control the motion of the first motor. However, the timer controlling the Arduino also requires pin 5. The shield has then been modified to control the stepping of motor 1 with pin 23. Motor 2 is controlled by pin 7 (direction) and pin 6 (stepping). In this version of the prototype, the step size was set to full step to maximize the movement velocity. Please note that the shield limits the digital control to steps and direction only while the Polulu driver's digital stepping options are set through a DIP switch on the board. A trade-off exists between the resolution and velocity of movement. While microstepping down to 1/16 of the full step (~200 nm) is available with the Polulu drivers, the step size was set to the full step to maximize the velocity, as minimum polarization of the coil is needed for the movement of the motors.

Different protocols can be applied as depicted in Fig. 6(b): linear (stretch increase with time), static (stretch to a specific value for a specific period of time), and cyclic (stretch of a specific value and reverse during a specific period of time). Although a sinusoidal variation (red curves, bottom panel) could be programmed, only the triangular cyclic displacement has been implemented (blue line, bottom panel) for the current work.

Validation of the mechanical sub-system

Deformation of the membrane induced by the displacement of the motor was studied based on the deformation of the seeding area borders. The results are presented in Fig. 7(a) where the width (W) and length (L) of the membrane seeding area [(measures were taken as highlighted in panel (b)] are shown for stretch and return phases (note that the values for the return phase is shown with the inverse sign for clarity). There is a linear relationship between the displacement of the motors using the control center (Arduino-based system) and the actual deformation applied to the membrane [Fig. 7(a)]. As such, a displacement of 6 mm is transduced to a strain of 31.04% of the membrane seeding area in the direction of the displacement [example shown in panel (b)]. However, a small decrease (−6.7%) in the membrane width (perpendicular direction of the displacement) was observed. This contraction in the width of the membrane can be explained by the Poisson effect. The calculated Poisson ratio

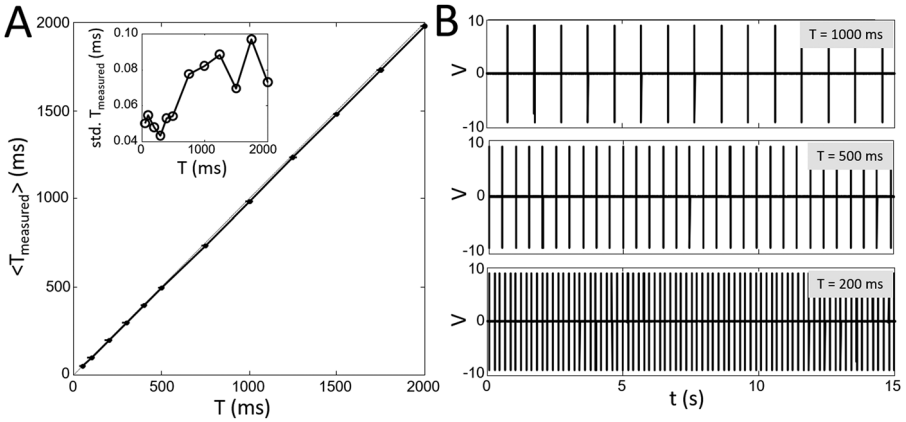

FIG. 5. (a) Comparison between the programmed stimulation period (T) and the average measured period of stimulation ($\langle T_{measured} \rangle$) showing a clear and stable 1:1 response with very narrow standard deviation error bars corresponding to the values shown in the inset. Test pulses had 2 ms positive and negative bipolar duration. (b) Three examples of signals obtained for T = 1 s (top), T = 0.5 s (middle), and T = 0.2 s (bottom) stimulation period.

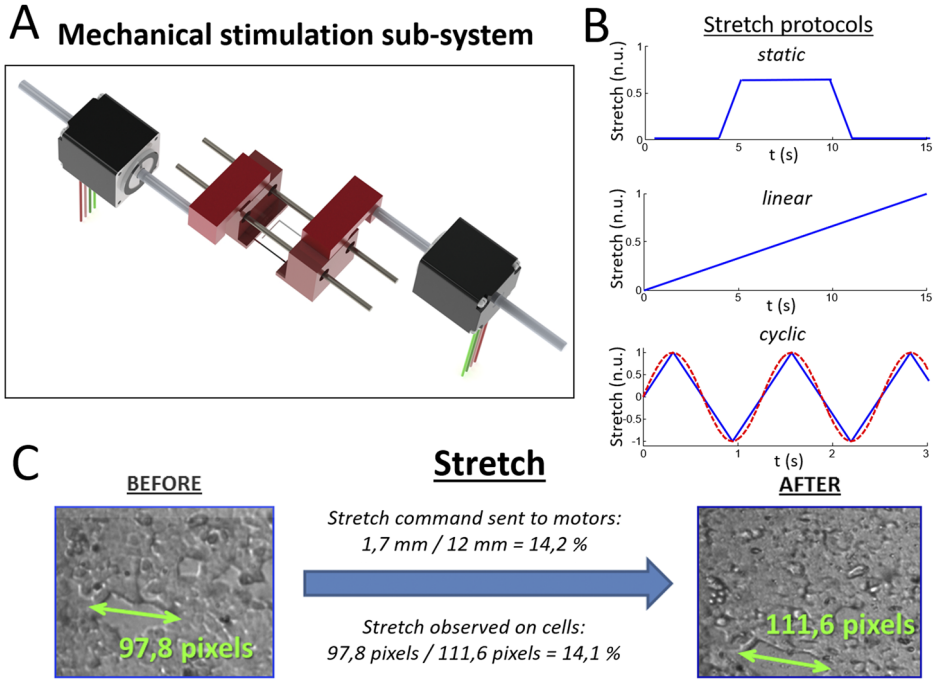

FIG. 6. Mechanical stimulation sub-system characteristics. (a) Schematic of the sub-system setup based on two linear stepper motors that move two membrane holders to which the PDMS membrane is attached. Two stainless steel rods serve as a guiding rail for the displacement along the longer axis of the membrane. (b) Sketch of the different mechanical protocols that can be used with our design, including static (top), linear (middle), and cyclic (bottom). Combinations of these different protocols could easily be integrated for complex culture protocols. (c) Example of applied deformation of attached Hek293t cells on the displacement of the motors by 1.7 mm resulting to a 14.2% stretch increase.

for a 6 mm stretch was 0.22. Return from the stretched to the initial state shows also a linear relationship between the motor displacement and stretch level. However, a comparison of the absolute value of the regression slope highlights a slight difference (5.4%/mm for the stretching phase vs 5.7%/mm for the return phase). Preliminary evaluations suggest that the mechanical construction needs to have a lower tolerance than what was tested for this prototype.

Cyclic stretch is an important modulator of cardiomyocyte electrophysiological and contractile characteristics. As such, our proposed design offers the possibility of various mechanical stimulation types, including a cyclic stretch protocol. Cyclic

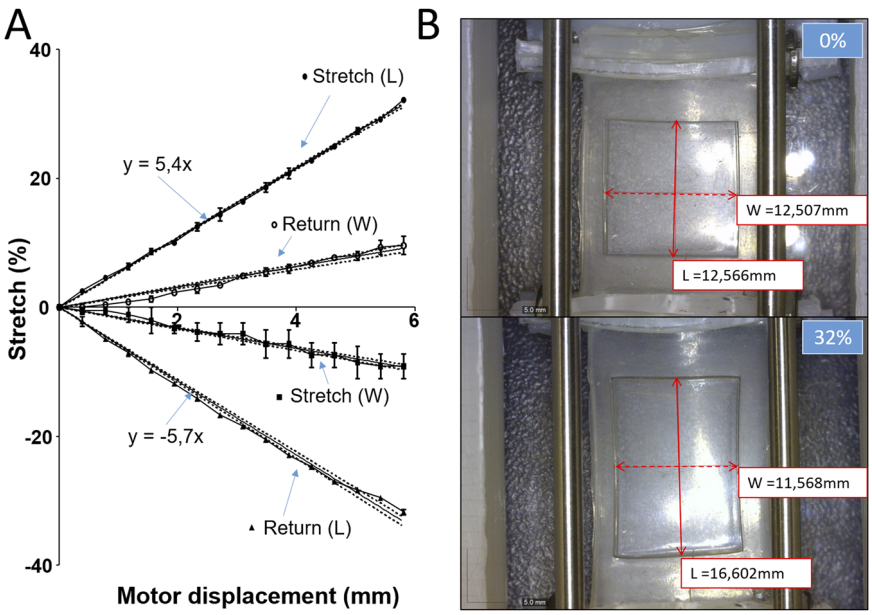

FIG. 7. Study of the link between the motor displacement and cell seeding region. (a) A linear relationship exists between the motor shaft displacement (for values between 0 mm and 6 mm) for both the stretching and return phases (from the stretched state to the unstretched state). The second set of lines corresponds to the transverse change in the template where contraction is seen while stretching the membrane. (b) Example of the data obtained and analyzed to obtain the results presented in panel (a) where a displacement of 6 mm resulted in 32% stretch and 8% contraction in the transverse axis.

modulation of the length (L) and width (W) of the cell seeding template has been studied [see the definition in Fig. 8(a)]. An example of cyclic variation in the top and bottom boundary of the template is shown in panel (B-i), while cyclic contraction due to the Poisson effect is found along the axis orthogonal to the stretch [panel (B-ii)]. The measured period of the cycle ($\langle T_{measured} \rangle$) has been tested over a range of imposed period (T) and the results are shown in Fig. 8(c). As expected, a 1:1 relationship with very low variability was found, confirming the stability and reliability of the approach.

Important procedural steps in culturing cardiomyocytes with electrical and mechanical stimulations

As in any cell culture setup, careful cleaning and sterile conditions are central. The BioR is an assembly of several parts. Thus, maintaining appropriate sterile conditions, including cleaning procedures, is more challenging than that for regular cell culture in petri dishes. A series of important steps have been determined. Every individual part must be cleaned with dishwashing or specialized soap (e.g., Decon 90, Decon Laboratories Limited, England) to remove dust and residue from previous culture activity. All parts are then put in 1% Javel-deionized water for 24 h to make sure that the porous material is thoroughly decontaminated (including carbon electrodes). The components are then washed out and immersed in deionized water for 24 h, changed with fresh water every 6 h (at least three times over the 24 h period). The components are then sterilized by ethylene oxide, a sterilization process compatible with ABS components of the system. The parts can be re-assembled and connected to the motors under a sterile hood. Coating (to improve adhesion of the cells) is added on the PDMS membrane. Either a combination of gelatin/fibronectin[39] or fibronectin alone[40] was found to enhance the formation of a homogeneous monolayer. The assembled system is then exposed to UV light for 15 min under sterile hood. The sterilized system can then be put in the incubator, ready for cell seeding.

Tests performed with rat neonatal cardiomyocytes suggest that a relatively high density of cells is required to obtain a good syncytium on the PDMS template within 24–48 h. A density of 450 000 cells/cm^2 usually provides a monolayer with synchronized activity (in the absence of mechanical and electrical stimulations). It is worth noting that the key step is a 3-h resting period following cell seeding, before adding cell culture media or moving the system. This step is essential to maximize the yield and homogeneous dispersion of cells within the membrane template.

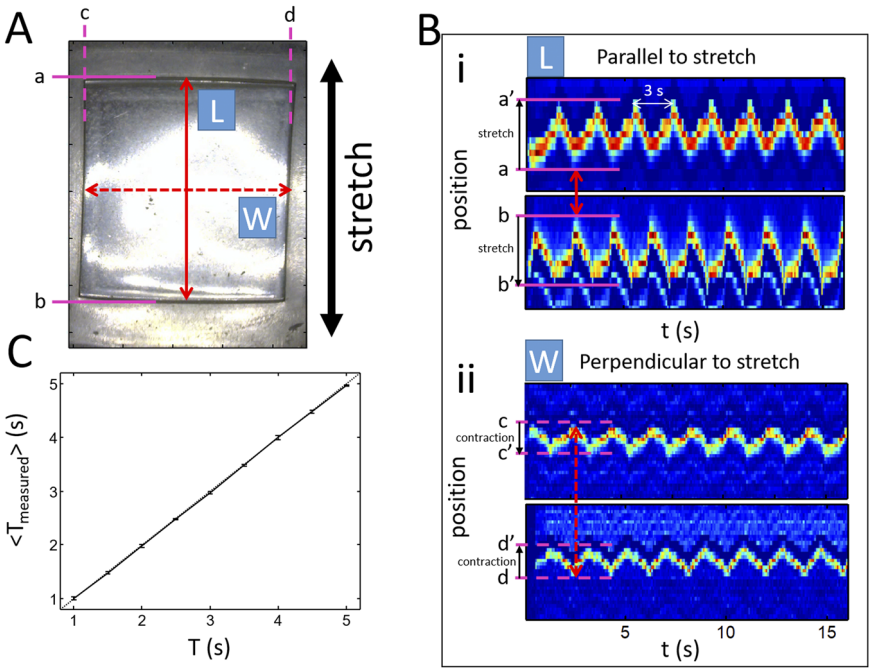

FIG. 8. Evaluation of the BioR cyclic stretch. (A) Image of the cell seeding region with the definition of the length (L, along the direction of stretch) and width (W, transverse to the stretch). The boundaries (for the cell seeding region) , which are displaced in the direction of stretch are labeled a and b (magenta continuous lines) and, which are displaced perpendicular to the stretch (contraction displacement) are labeled c and d (magenta dashed lines). (B) Example of cyclic stretch with a period of T = 3 s and ~8% stretch shown as a color scale (boundaries are detected as a gradient of light intensity) is shown in colors (from cyan to red) over time. (B-i) Stretch of the boundary a (top, pre-stretch position a and stretched position a′) of L and boundary b (bottom, pre-stretch position b and stretched position b′). (B-ii) Contraction of the boundary c (top, pre-stretch position c and stretched position c′) and boundary d (bottom, pre-stretch position d and stretched position d′) along W. (C) Comparison between the measured average periods ($\langle T_{measured} \rangle$) vs the imposed periods of cyclic stretch showing a clear match with a very limited timing error (error bars represent the standard deviation) over a 30 s recording.

DISCUSSION AND CONCLUSION

We have designed and built a bioreactor prototype that incorporates both mechanical and electrical stimulations. The main interest in our approach is the fine control of the stimulation parameters in regard to timing and amplitude, within a "simple" design consisting of easy to find, affordable components and 3D printable parts. This approach opens the way to more complex protocols for electrical and/or mechanical stimulations.

Electrical stimulation can be applied either through localized bipolar stimulation[41] or field stimulation.[42] We opted for the field stimulation approach to promote synchronized excitation of cells since localized stimulation (either unipolar or bipolar) directly stimulates a limited number of cells proximal to the electrodes. Moreover, activation is dependent on the cell confluence level as well as intercellular electrical coupling between cells. Various patterns of electrical stimulation can be generated involving different pacing periods. This is an important feature since progressively increased frequency has been reported to induce electrophysiological changes consistent with cardiac cell maturation.[5] Interestingly, the system allows the programming of irregular stimulation periods, which is known to contribute significantly to ventricular excitation–contraction coupling by altering the expression and activity of key calcium-handling proteins.[43]

The innovative design of the culture membrane, including a specialized region for cell seeding is customizable (using different molds) in order to satisfy particular requirements and optimize optical mapping studies. Mechanical stimulation is known to modulate functional properties of cardiomyocytes and is also believed to be a key factor to promote optimized adult phenotype of derived-cardiomyocytes.[5] Although pulsatile linear stretch *in vitro* causes marked upregulation of proteins that form electrical and mechanical junctions[44] and acute linear stretch was shown to affect the action potential duration[45] or inducing myocyte hypertrophy,[46] the specific outcomes upon application of different stretch types still remains to be determined. Furthermore, complex stretching patterns have been proposed to mimic *in vivo* tissue contraction.[47] Several methods can be used to apply mechanical stimulation to cells: axial stretch using carbon fibers,[48] unidirectional stretch using an elastic substrate,[46] and biaxial stretch of elastic substrate.[49,50] While biaxial stretch is the most physiologically relevant deformation, uniaxial stretch implemented in our prototype remains interesting but can be limited in part by its Poisson contraction.

Uniaxial stretch has been applied through motor-induced rotation of an elliptical rod/wheel[44,51] or by a single electric motor[52,53] or pneumatic actuator deforming an elastic membrane or cells-embedded construct.[54] Spatially constrained deformation by pressure variation underneath a sealed membrane can also apply stretch to cells.[55] Even fluid jet applied to cardiomyocytes has been proposed to study the effect of acute stretch.[55] Of interest is the application of dielectric elastomer actuator, which can deform using high voltage thus applying stretch to attached cells[56] to which extracellular electrodes can be incorporated for measurement of cell electrical activity.[57] A specificity of our concept is the use of two motors in order to apply the unidirectional stretch. The decision was made from the beginning in order to facilitate imaging the samples during the culture process. The center of the membrane remains stable when the same displacement is imposed to the motors (but in the opposite direction) and, as such, keeping the field of view stable when centered at the middle of the membrane. However, we believe that the use of two motors has an added value as to be able to re-position the membrane, if needed without changing the elongation state of the membrane by applying a displacement of the motor in the same direction. This characteristic of our concept could thus easily permit imaging at higher resolution along the axis of deformation without additional hardware.

As expected, the motors, when in use, generate heat. When testing the prototype in the incubator (Thermo Forma Series II incubator), we found that an adaptation time was needed to obtain a stable temperature because of heat generated by the motors. We tested and concluded that a period of "training" of 30 min with cyclic elongation at 0.5 Hz (without the culture membrane) was long enough to stabilize the temperature (when read on the incubator display) and kept constant over the test period of 24 h for culture for the same cyclical stretch protocol. Increasing the number of bioreactors in the incubator may, however, be limited as many incubators are designed to control heating but not cooling. To circumvent this possible limitation, the use of a liquid cooling system attached to the motors with the heat sink located outside the incubator should be considered.

A culture incubator is a harsh environment for electronics and motors. Although no problem has been identified with the current motor choice, the alternative could be considering to favor a longer longevity of the system. The best options should be selecting IP65 certified stepper motors. As an intermediate step, application of a silicone spray sealer on the motors and the polarization leads could be considered.

As in all cell culture procedures, special care is needed. Specific timing for electrical and mechanical stimulation initiation is important as highlighted above. Adhesion of cells to the membrane is crucial to the approach where strain of an elastic membrane is transferred to cells. A pre-culture time of 3–5 days after seeding the neonatal rat cardiomyocytes is optimal prior electrical stimulation. The culture medium should be changed daily to minimize potential accumulation of charges and wastes in the culture[9] although continuous medium change could improve the control of factors, including autocrine modulators.

Our future aim is to use this system with induced pluripotent stem cells to enhance differentiation and preservation of cardiac phenotype as it would require precise electrical and mechanical stimulations. The system described here would allow to study and optimize tissue engineered cardiac patches with improved contractility, controlled spontaneous rate of activity (as in the biopacemaker concept[58,59]), modulated responses to cholinergic (modulation of spontaneous activity) and adrenergic stimulation (modulation of spontaneous activity and contractility), or decreased automaticity to limit arrhythmia.

ACKNOWLEDGMENTS

This work was supported by the Montreal Heart Institute Foundation, the Natural Sciences and Engineering Research Council of Canada, and the Fondation Institut de Cardiologie de Montréal.

There is no potential conflict of interest to disclose.

REFERENCES

[1] A. E. Moran *et al.*, "Temporal trends in ischemic heart disease mortality in 21 world regions, 1980-2010: The Global Burden of Disease 2010 study," Circulation **129**(14), 1483–1492 (2014).
[2] J. Zhang *et al.*, "Functional cardiomyocytes derived from human induced pluripotent stem cells," Circ. Res. **104**(4), e30–e41 (2009).
[3] L. Wang *et al.*, "Stoichiometry of Gata4, Mef2c, and Tbx5 influences the efficiency and quality of induced cardiac myocyte reprogramming," Circ. Res. **116**(2), 237–244 (2015).
[4] N. L. Tulloch *et al.*, "Growth of engineered human myocardium with mechanical loading and vascular coculture," Circ. Res. **109**(1), 47–59 (2011).
[5] S. S. Nunes *et al.*, "Biowire: A platform for maturation of human pluripotent stem cell-derived cardiomyocytes," Nat. Methods **10**(8), 781–787 (2013).
[6] C. P. Jackman *et al.*, "Human cardiac tissue engineering: From pluripotent stem cells to heart repair," Curr. Opin. Chem. Eng. **7**, 57–64 (2015).
[7] A. Sathaye *et al.*, "Electrical pacing counteracts intrinsic shortening of action potential duration of neonatal rat ventricular cells in culture," J. Mol. Cell. Cardiol. **41**(4), 633–641 (2006).
[8] Z. Yang *et al.*, "Rapid stimulation causes electrical remodeling in cultured atrial myocytes," J. Mol. Cell. Cardiol. **38**(2), 299–308 (2005).
[9] N. Tandon *et al.*, "Optimization of electrical stimulation parameters for cardiac tissue engineering," J. Tissue Eng. Regener. Med. **5**(6), e115–e125 (2011).
[10] S. Rangarajan, L. Madden, and N. Bursac, "Use of flow, electrical, and mechanical stimulation to promote engineering of striated muscles," Ann. Biomed. Eng. **42**(7), 1391–1405 (2014).
[11] G. Kensah *et al.*, "A novel miniaturized multimodal bioreactor for continuous in situ assessment of bioartificial cardiac tissue during stimulation and maturation," Tissue Eng., Part C **17**, 463 (2011).
[12] P. Taggart *et al.*, "Developing a novel comprehensive framework for the investigation of cellular and whole heart electrophysiology in the in situ human heart: Historical perspectives, current progress and future prospects," Prog. Biophys. Mol. Biol. **115**, 252 (2014).
[13] T. Keller and A. Kuhn, "Electrodes for transcutaneous (surface) electrical stimulation," J. Autom. Control **18**(2), 35–45 (2008).
[14] H. Plenk, Jr., "The role of materials biocompatibility for functional electrical stimulation applications," Artif. Organs **35**(3), 237–241 (2011).
[15] P. Zhang *et al.*, "Low-voltage direct-current stimulation is safe and promotes angiogenesis in rabbits with myocardial infarction," Cell Biochem. Biophys. **59**(1), 19–27 (2011).
[16] P. M. De Paula *et al.*, "Hemodynamic responses to electrical stimulation of the aortic depressor nerve in awake rats," Am. J. Physiol. **277**(1 Pt 2), R31–R38 (1999).
[17] M. Grobety, D. Sedmera, and L. Kappenberger, "The chick embryo heart as an experimental setup for the assessment of myocardial remodeling induced by pacing," Pacing Clin. Electrophysiol. **22**(5), 776–782 (1999).
[18] B. Schwaab *et al.*, "Chronic ventricular pacing using an output amplitude of 1.0 volt," Pacing Clin. Electrophysiol. **20**(9 Pt 1), 2171–2178 (1997).
[19] Y. Xiao *et al.*, "Microfabricated perfusable cardiac biowire: A platform that mimics native cardiac bundle," Lab Chip **14**(5), 869–882 (2014).
[20] L. Lu *et al.*, "Design and validation of a bioreactor for simulating the cardiac niche: A system incorporating cyclic stretch, electrical stimulation, and constant perfusion," Tissue Eng., Part A **19**(3-4), 403–414 (2013).
[21] Y. Barash *et al.*, "Electric field stimulation integrated into perfusion bioreactor for cardiac tissue engineering," Tissue Eng., Part C **16**(6), 1417–1426 (2010).
[22] C. Nick *et al.*, "Three-dimensional carbon nanotube electrodes for extracellular recording of cardiac myocytes," Biointerphases **7**(1-4), 58 (2012).
[23] U. Nussinovitch and L. Gepstein, "Optogenetics for in vivo cardiac pacing and resynchronization therapies," Nat. Biotechnol. **33**(7), 750–754 (2015).
[24] S. B. Knisley and B. C. Hill, "Effects of bipolar point and line stimulation in anisotropic rabbit epicardium: Assessment of the critical radius of curvature for longitudinal block," IEEE Trans. Biomed. Eng. **42**(10), 957–966 (1995).
[25] L. Tung, N. Sliz, and M. R. Mulligan, "Influence of electrical axis of stimulation on excitation of cardiac muscle cells," Circ. Res. **69**(3), 722–730 (1991).
[26] M. Radisic *et al.*, "Functional assembly of engineered myocardium by electrical stimulation of cardiac myocytes cultured on scaffolds," Proc. Natl. Acad. Sci. U. S. A. **101**(52), 18129–18134 (2004).
[27] S. Pietronave *et al.*, "Monophasic and biphasic electrical stimulation induces a precardiac differentiation in progenitor cells isolated from human heart," Stem Cells Dev. **23**(8), 888–898 (2014).
[28] R. S. Martherus *et al.*, "Electrical signals affect the cardiomyocyte transcriptome independently of contraction," Physiol. Genomics **42A**(4), 283–289 (2010).
[29] P. Di Nardo *et al.*, "Myocardial expression of atrial natriuretic factor gene in early stages of hamster cardiomyopathy," Mol. Cell. Biochem. **125**(2), 179–192 (1993).
[30] H. J. Berger *et al.*, "Continual electric field stimulation preserves contractile function of adult ventricular myocytes in primary culture," Am. J. Physiol. **266**(1 Pt 2), H341–H349 (1994).
[31] D. Tremblay *et al.*, "A novel stretching platform for applications in cell and tissue mechanobiology," J. Visualized Exp. **88**, e51454 (2014).
[32] J. G. Jacot *et al.*, "Mechanostransduction in cardiac and stem-cell derived cardiac cells," in *Mechanosensitivity of the Heart* (Springer, 2010), pp. 99–139.
[33] P. Kohl, F.Sachs, and M. R. Franz, *Cardiac Mechano-Electric Coupling and Arrhythmias*, 2nd ed.(Oxford University Press, Oxford, 2011), p. 477.
[34] F. Gannier *et al.*, "A possible mechanism for large stretch-induced increase in $[Ca^{2+}]$i in isolated guinea-pig ventricular myocytes," Cardiovasc. Res. **32**(1), 158–167 (1996).
[35] A. Buccarello *et al.*, "Uniaxial strain of cultured mouse and rat cardiomyocyte strands slows conduction more when its axis is parallel to impulse propagation than when it is perpendicular," Acta Physiol. **223**(1), e13026 (2018).
[36] J. E. Saffitz and A. G. Kleber, "Effects of mechanical forces and mediators of hypertrophy on remodeling of gap junctions in the heart," Circ. Res. **94**(5), 585–591 (2004).
[37] X. Q. Brown, K. Ookawa, and J. Y. Wong, "Evaluation of polydimethylsiloxane scaffolds with physiologically-relevant elastic moduli: Interplay of substrate mechanics and surface chemistry effects on vascular smooth muscle cell response," Biomaterials **26**(16), 3123–3129 (2005).
[38] A. L. Thangawng *et al.*, "An ultra-thin PDMS membrane as a bio/micro-nano interface: Fabrication and characterization," Biomed. Microdevices **9**(4), 587–595 (2007).
[39] J. Boudreau-Beland *et al.*, "Spatiotemporal stability of neonatal rat cardiomyocyte monolayers spontaneous activity is dependent on the culture substrate," PLoS One **10**(6), e0127977 (2015).
[40] N. Badie *et al.*, "Conduction block in micropatterned cardiomyocyte cultures replicating the structure of ventricular cross-sections," Cardiovasc. Res. **93**(2), 263–271 (2012).
[41] V. Munoz *et al.*, "Adenoviral expression of IKs contributes to wavebreak and fibrillatory conduction in neonatal rat ventricular cardiomyocyte monolayers," Circ. Res. **101**(5), 475–483 (2007).
[42] N. Tandon *et al.*, "Alignment and elongation of human adipose-derived stem cells in response to direct-current electrical stimulation," Conf. Proc. IEEE Eng. Med. Biol. Soc. **1**, 6517–6521 (2009).
[43] L. H. Ling *et al.*, "Irregular rhythm adversely influences calcium handling in ventricular myocardium: Implications for the interaction between heart failure and atrial fibrillation," Circ.: Heart Failure **5**(6), 786–793 (2012).
[44] J. Zhuang *et al.*, "Pulsatile stretch remodels cell-to-cell communication in cultured myocytes," Circ. Res. **87**(4), 316–322 (2000).
[45] T. L. Riemer and L. Tung, "Stretch-induced excitation and action potential changes of single cardiac cells," Prog. Biophys. Mol. Biol. **82**(1-3), 97–110 (2003).
[46] J. Sadoshima *et al.*, "Molecular characterization of the stretch-induced adaptation of cultured cardiac cells. An in vitro model of load-induced cardiac hypertrophy," J. Biol. Chem. **267**(15), 10551–10560 (1992).
[47] J. J. Lau, R. M. Wang, and L. D. Black III, "Development of an arbitrary waveform membrane stretcher for dynamic cell culture," Ann. Biomed. Eng. **42**(5), 1062–1073 (2014).
[48] J. Y. Le Guennec *et al.*, "A new method of attachment of isolated mammalian ventricular myocytes for tension recording: Length dependence of passive and active tension," J. Mol. Cell. Cardiol. **22**(10), 1083–1093 (1990).

[49]O. R. Rana *et al.*, "A simple device to apply equibiaxial strain to cells cultured on flexible membranes," Am. J. Physiol.: Heart Circ. Physiol. **294**(1), H532–H540 (2008).
[50]A. A. Lee *et al.*, "An equibiaxial strain system for cultured cells," Am. J. Physiol. **271**(4 Pt 1), C1400–C1408 (1996).
[51]C. Fink *et al.*, "Chronic stretch of engineered heart tissue induces hypertrophy and functional improvement," FASEB J. **14**(5), 669–679 (2000).
[52]Y. Huang *et al.*, "Effect of cyclic strain on cardiomyogenic differentiation of rat bone marrow derived mesenchymal stem cells," PLoS One **7**(4), e34960 (2012).
[53]K. Naruse, T. Yamada, and M. Sokabe, "Involvement of SA channels in orienting response of cultured endothelial cells to cyclic stretch," Am. J. Physiol. **274**(5), H1532–H1538 (1998).
[54]J. W. Miklas *et al.*, "Bioreactor for modulation of cardiac microtissue phenotype by combined static stretch and electrical stimulation," Biofabrication **6**(2), 024113 (2014).
[55]B. Husse *et al.*, "Cyclical mechanical stretch modulates expression of collagen I and collagen III by PKC and tyrosine kinase in cardiac fibroblasts," Am. J. Physiol.: Regul., Integr. Comp. Physiol. **293**, R1898 (2007).
[56]J. Costa *et al.*, "Bioreactor with electrically deformable curved membranes for mechanical stimulation of cell cultures," Front. Bioeng. Biotechnol. **8**, 22 (2020).
[57]M. Imboden *et al.*, "High-speed mechano-active multielectrode array for investigating rapid stretch effects on cardiac tissue," Nat. Commun. **10**(1), 834 (2019).
[58]J. E. Duverger *et al.*, "Multicellular automaticity of cardiac cell monolayers: Effects of density and spatial distribution of pacemaker cells," New J. Phys. **16**(11), 113046 (2014).
[59]J. B. Béland, J. E. Duverger, and P. Comtois, "Génie tissulaire appliqué à l'activité électrique cardiaque autonome: Une alternative au pacemaker électronique?," Médecine/Sciences Amérique **2**(2), 1 (2013) ["Tissue engineering applied to cardiac autonomous activity: An alternative to electronic pacemaker?," Med Sci (Paris) **26**(1), 57–64 (2010)].